Dermatan Sulfate Epimerase 1-Deficient Mice have Reduced Content and Changed Distribution of Iduronic acids in Dermatan Sulfate and an Altered Collagen Structure in Skin

Marco Maccarana[1*], Sebastian Kalamajski[2], Mads Kongsgaard[3], S. Peter Magnusson[3], Åke Oldberg[2], and Anders Malmström[1]

[1,2]Department of Experimental Medical Science, Biomedical Center D12[1], and B12[2], Lund University, SE-221 84 Lund, Sweden.
[3]Institute of Sports Medicine, Bispebjerg Hospital, Bispebjerg Bakke 23, DK 2400 Copenhagen NV, Denmark.

Running title: FUNCTION OF DERMATAN SULFATE

**Address correspondence to: Marco Maccarana, Department of Experimental Medical Science, Biomedical Center D12, Lund University, SE-221 84 Lund, Sweden*
Tel. +46 46222 9665; Fax +46 46211 3417; E-mail marco.maccarana@med.lu.se

Dermatan sulfate epimerase 1 (DS-epi1) and 2 convert glucuronic acid to iduronic acid in chondroitin/dermatan sulfate biosynthesis. Here we report on the generation of DS-epi1-null mice and the resulting alterations in the chondroitin/dermatan polysaccharide chains. The numbers of long blocks of adjacent iduronic acids are greatly decreased in skin decorin and biglycan chondroitin/dermatan sulfate, along with a parallel decrease of iduronic-2-O-sulfated-galactosamine-4-O-sulfated structures. Both iduronic acid blocks and iduronic acids surrounded by glucuronic acids are also decreased in versican-derived chains. DS-epi1-deficient mice are smaller than wild-type littermates, but otherwise have no gross macroscopic alterations. The lack of DS-epi1 affects the chondroitin/dermatan sulfate in many proteoglycans and the consequences for skin collagen structure were initially analyzed. We found that the skin collagen architecture was altered, and electron microscopy showed that the DS-epi1-null fibrils have a larger diameter than the wild-type fibrils. The altered chondroitin/dermatan sulfate chains carried by decorin in skin are likely to affect the collagen fibril formation and reduce the tensile strength of DS-epi1-null skin.

Chondroitin sulfate (CS) is an unbranched polymer chain composed of alternating glucuronic acid (GlcA) and N-acetyl galactosamine (GalNAc) (36,49). In dermatan sulfate (DS) D-glucuronic acid is converted to its epimer L-iduronic acid (IdoA) (25). The extent of this modification, which varies from a few percent of the glucuronic acid being epimerized to a predominant presence of iduronic acid, depends on the variable epimerase activity in tissues and on the core protein attached to the chain in CS/DS-proteoglycans (PG) (41,47). The same CS/DS-proteoglycan has different content of iduronic acid depending on the cell type and tissue of origin (4,5). The name CS/DS denotes the hybrid GlcA-IdoA nature of the chain. It has long been known that the distribution of iduronic acids within the chain is not random but follows two patterns: either they are clustered together, forming long iduronic acid blocks, or they are isolated, i.e. interspersed among surrounding glucuronic acid (11). Dermatan sulfate epimerase 1 and 2, in short DS-epi1 and DS-epi2, encoded in mouse by *Dse* and *Dsel(like)* genes, respectively, are present from Xenopus tropicalis to humans but not in worms and fly (23,34). During DS biosynthesis, epimerization is followed by the action of eight C-specific *O*-sulfotranferases, which transfer a sulfate group to C-2 of both IdoA and GlcA, and to C-4, C-6, C-4/C-6 of GalNAc (18). These modification reactions, individually affecting only part of the available substrate, produce structural variability in the CS/DS chain. Considerable efforts have been made to characterize specific sequences in the CS/DS chains responsible for binding to protein, and the subsequent mediation of a biological effect (28). For instance (IdoA-2OS-GalNAc-4OS)$_3$ and GalNAc-4/6-diOS-containing structures bind and activate heparin

cofactor II, which is the major antithrombotic system in the subendothelial layer (48). IdoA/GlcA-2OS-GalNAc-6OS-containing structures bind to pleiotrophin, mediating neuritogenic activity (3,44). IdoA-GalNAc-4OS-containing structures bind to basic fibroblast growth factor and the complex has been shown to be active in wound healing (46).

CS/DS-PGs are mainly found in the extracellular matrix (ECM). They belong to four families: lecticans; e. g. versican, aggrecan, brevican and neurocan; collagens: e. g. collagen IX; basement membrane proteoglycans: e. g. SMC3, collagen XV, perlecan, containing both heparan sulfate and CS/DS; Small Leucine-rich Repeat Proteoglycans (SLRP). Some proteoglycans of the first three groups are referred to as CS-PGs. The actual presence of iduronic acid, depending on the tissue examined and on the developmental stage, has been overlooked in many cases (37,44). The archetypical SLRP family members, decorin, biglycan, fibromodulin and lumican, bind fibrillar collagens and affect the collagen fibril and scaffold formation in connective tissues (15). Decorin and biglycan are substituted with one and two CS/DS chains, respectively. Decorin is involved in collagen type I fibril formation and matrix assembly in a wide range of connective tissues and binds near the C-terminus of collagen monomers delaying their accretion to the growing fibrils. We have identified an SYIRIADTNIT sequence in decorin as essential for binding to collagen (16). The role of the decorin CS/DS chain *in vivo* has not been explored, although *in vitro* studies suggest that IdoA promotes the binding of CS/DS to collagen (31) and is required for self-association of CS/DS chains (6,10,22).

Here the function of DS-epi1 in mice was disrupted. DS-epi1-deficient mice show CS/DS with a marked deficiency in iduronic acid-containing structures. The deletion of DS-epi1 is likely to affect many types of proteoglycans and to result in a complex phenotype. We focus on skin alterations presumably caused by altered decorin/biglycan CS/DS chains.

MATERIALS AND METHODS

Materials - Cell culture reagents were from Invitrogen. Red-Separose gel, Superose 6 HR 10/30, Superdex Peptide 10/300 GL, and PD-10 columns, ECL-Plus reagent were from GEHealthcare. DE52 anion exchange gel was from Whatman. $^{35}SO_4$ (1500 Ci/mmol) was from PerkinElmer. Chondroitinase ABC, B, and AC-I were from Seigakaku. Brilliant blue G colloidal gel-staining solution was from Sigma.

Construction of the targeting vector and generation of chimeric mice - A genomic *Dse*/*Sart2* clone was isolated from a mouse genomic PAC library (RPCI21; Geneservice, Cambridge, UK) (33). A 6.3 kb SphI-StuI fragment was ligated in pBluescript II KS (Stratagene) and a phosphoglycerate kinase-neomycin resistance cassette (pGKNeo) (26) was inserted in the reverse transcriptional orientation in a unique XhoI site located in the second exon of *Dse*/*Sart2* (Fig. 1A). The targeting vector was linearized at a NotI site and used to transfect R1 mouse embryonic stem cells at Lund Transgenic Core Facility as described (45). Clones were picked and analyzed by southern blot after NcoI digestion using a 420 bp external probe. This probe hybridizes with a 6.3 kb wild type and a 4.8 kb Nco I

fragment (Fig. 1B). Three individually targeted clones were injected into C57BL/6 blastocysts to generate chimeric mice. Chimeric males were obtained from two clones and were mated with C57BL/6 females. F1 mice with germ line transmission were intercrossed to produce all genotypes in a mixed C57BL/6//129/SvJ genetic background. All experiments in this study were conducted on littermates of this mixed genetic background. Mice derived from two ES clones were characterized for: *i) Dse* allelic distribution at weaning, *ii) Dse* expression by qRT-PCR and by western blot, *iii)* shape at birth of the tail, and *iv)* weight measured between birth and weaning. Given the complete identity of the *Dse*-/- mice from the two ES clones, according to the above four criteria, only mice derived from one ES clone were further characterized. Mice were genotyped by PCR from tail DNA using the following primers: forward common for both alleles 5'-AGCACATTGCAGCTCGGCTTAC-3', reverse for wild-type allele 5'-GCTGCCATCCTCTCCATGTAGTC-3', reverse for neo-cassette mutated allele 5'-TGGATGTGGAATGTGTGCGAGG-3'. The use of animals for research complied with national guidelines, and permission was given by the regional ethical board.

Quantitative RT-PCR – Total RNA was extracted from tissues using RNAeasy kit (Qiagen), DNase-treated with DNA-free™ Kit (Applied Biosystems), and cDNA synthesis was performed with SuperScript® VILO™ cDNA synthesis kit (Invitrogen). The samples were mixed with primers and SYBR Green Master Mix (Applied Biosystems) and amplified in an ABI Prism instrument (Applied Biosystem, Foster City, CA) starting with an initial 2-min heating at 50°C and 10-min heating at 95°C followed by 40 cycles at 95°C for 15 s and 60°C for 60 s. The

data were analyzed using SDS 2.1 software (Applied Biosystems). The calculated threshold cycle (Ct) values were normalized to the Ct-value for glyceraldehyde-3-phosphate dehydrogenase (GAPDH). The primers used were *Dse*: 5'-TGTGTGCTGTATCCTGAGAACA -3' and 5'-CAAGGCGCATCTTTCACCAAC -3'; *GAPDH*: 5'-AGGTCGGTGTGAACGGATTTG-3' and 5'-TGTAGACCATGTAGTTGAGGTCA-3'.

Establishment of primary fibroblasts cell culture - Lung and skin fibroblasts were derived from 2-month-old animals. Small pieces of the organs were adhered to plastic and cultivated in MEM, 10%FBS. Outcoming cells were grown for 10 days and split (passage 1). Cells were utilized for the experiments between passage 4 and passage 7.

Western blot and immunohistochemistry - Cells were lysed in 20 mM MES pH 6.5, 150 mM NaCl, 10% glycerol, 2 mM DTT, 1 mM EDTA, 1% Triton X-100, protease inhibitors, i.e. PMSF 1mM, aprotinin leupeptin and pepstatin each at 1 µg/ml (lysis buffer). Spleen, lung, kidney, skin, and brain organs were homogenized in ~3-fold excess (v:w) of lysis buffer with the use of a Potter. Protein content was determined in cleared lysates by Bradford method (BioRad), using BSA as standard. Alternatively, 5-mg organ lysates were bound in batch to 50 µl of Red-Sepharose gel, incubated 60 min, washed 5 times with lysis buffer, and finally eluted by reducing Laemli sample buffer.

DS-epi1 was detected using 1µg/ml of an immunopurified anti-DS-epi1 rabbit polyclonal antibody obtained after antigen peptide immunization: (KWSKYKHDLAAS corresponding to aminoacid 509-520 of the human/murine

sequence), Innovagen, Sweden. ECL-Plus was used as HRP substrate. Immunohistochemistry was done as described (45) using antisera against decorin and biglycan**.**

DS-epimerase activity - 200 µl of organ or cell lysates were desalted using as dialysis buffer 20 mM MES (pH 5.5 at 37°C), 10% glycerol, 0.5 mM EDTA, 0.1% Triton X-100, 1 mM DTT, protease inhibitors. Protein content was determined after dialysis and equal amount of proteins of samples from the different genotypes were assayed for epimerase activity. The final assay volume was 100 µl of 0.8 X dialysis buffer, 2 mM $MnCl_2$, 0.5% NP40, and 30,000 dpm of the labeled chondroitin substrate ([5-^{3}H]defructosylated K4, prepared according to (14)). Incubations were carried out at 37°C for 20 h and the released tritium was quantified as described in (23).

Preparation of *in vivo* labeled CS/DS – Ten-day-old mice were i.p. injected with 50µl PBS, containing 200µCi $^{35}SO_4$, and kept alive for two h before sacrifice. To assess the structure of the CS/DS chains from the whole body, the entire mice were cut in pieces and grinded in 30 ml of 100mM Tris pH 8.5 (at 55°C), 200 mM NaCl, 5 mM EDTA buffer. The mixture was made 0.1% SDS, proteinase K was added till final 100µg/ml, and incubated at 55°C overnight. Further proteinase was added to cleared material and the incubation was continued for additional 6 h. The material was diluted 1:4 with 200 mM acetate pH 5.5, bound in batch with 1 ml DE-52 anion exchange, washed with 50mM acetate pH 5.5, 200 mM NaCl, eluted with 50 mM acetate pH 5.5, 1.5 M NaCl, added 10 µg CS-6-sulfated as carrier, and desalted using PD-10 column run in water. GAG chains were cleaved by ß-elimination in

50mM KOH, 100 mM $NaBH_4$ at 45ºC for 16-18 h and re-isolated again on DE-52 operated in principle as above. Heparan sulfate chains were depolymerised by deamination reaction at pH 1.5 (43), followed by re-isolation of CS/DS chains on Superose 6 run in 0.2 M NH_4HCO_3.

Preparation of labeled skin decorin/biglycan- and versican-CS/DS chains. Skin from 10-day-old mice, labeled as above, was extracted by Potter homogenization in 10 volumes (v/w) of guanidine 4M, 50 mM acetate pH 5.8, 10mM EDTA, 5 mM NEM, protease inhibitors. Cleared extracted material was dialized versus excess of 6M urea, 50 mM acetate pH 5.5, 0.2M NaCl, 1 mM EDTA, protease inhibitors. After dialysis, Triton was added till 0.1% and PG were bound to DE-52 gel, washed with dialysis buffer, 0.1% Triton, and eluted by 4M guanidine, 50 mM acetate pH 5.8, 10mM EDTA. 100µg dextran T500 was added as carrier, and PGs were size-separated on a Superose 6 column, run in 4M guanidine, 50 mM acetate pH 5.8, 10m M EDTA, 0.1% Triton. 10 µg CS-6-sulfated was added as carrier, and the isolated PGs were desalted by PD-10 columns run in water, and the GAG chains were cleaved from the core protein by β-elimination , re-purified on DE-52, freed from HS, and finally recovered, as described above.

Preparation of unlabeled skin decorin/biglycan – Skin from 3- to 4-month-old mice was extracted in guanidine-containing buffer, dialyzed versus urea-containing buffer and DE-52 purified as above. DE-52 purified material, without addition of any carrier, was ethanol-precipitated and run on Superose 6 as above, without addition of any carrier. Elution fractions were analyzed by western blot with anti-biglycan and anti-decorin antibodies. Pooled material was dialyzed stepwise versus

Hepes 50 mM pH 7.4, NaCl 0.15 M solutions containing decreasing concentration of urea (6 M, 3 M, no urea), and finally extensively versus water. Samples were lyophilized and resuspended in PBS. Most of the material was soluble, as it was recovered in the supernatant after 20,000 x g centrifugation. Purity was verified by SDS-PAGE (see Fig. 9).

Chondroitinases treatment of CS/DS and analysis of the split products – Cleavage of CS/DS chains by lyases (Seikagaku), as well as their analyses, were according to (34).

Collagen staining – Tissues were fixed in 95% ethanol, 1% acetic acid and decalcified in 6% EDTA in phosphate-buffered saline for 1 week prior to dehydration and embedding. Sections were stained with Chromotrope 2R and Sirius Red (Sigma).

Electron microscopy – Tissues from 3-month-old wild-type and *Dse*-/- mice were analyzed by transmission electron microscopy. After fixation in 0.15 M sodium cacodylate-buffered 2.5% glutaraldehyde, and post-fixation in 0.1 M *s*-collidine-buffered 2% osmium tetroxide, samples were embedded in epoxy resin. Ultrathin sections were analyzed in a Philips CM-10 electron microscope, and collagen fibril diameters were quantified with ImageJ software (NIH). To calculate fibril density the area occupied by collagen fibrils was measured by converting the image into black (collagen fibrils) and white (empty area) pixels, and their concurrent quantification was performed using ImageJ software (NIH). The Mann–Whitney U test was used to calculate significance, with $P < 0.05$ considered statistically significant (32).

Differential scanning calorimetry - Differential scanning calorimetry measurements were performed with either dissected skin, or with acid-solubilized collagen (Vitrogen) preincubated for 4 h in 37ºC in PBS in presence of extracted decorins from wild-type or *Dse*-/- mice. The thermograms were recorded in VP-DSC (MicroCal), scan rate 0.25°C/min, and medium feedback. Each thermogram was corrected by subtraction of a linear baseline based on a blank buffer sample, and normalized for collagen concentration.

Collagen fibrillogenesis assay – Acid-solubilized collagen (Vitrogen) was neutralized and diluted (100 µg/mL) in 150 mM NaCl, 20 mM HEPES, pH 7.4, with decorin extracted from wild-type or *Dse*-/- mice (2 µg/ml). Solutions were degassed and then incubated at 37°C in a spectrophotometer where the absorbance was continuously recorded at 400 nm.

Tensile strength determination. Dorsal skin samples from 5-month-old *Dse*-deficient (n=5) and wild type (n=5) mice were harvested immediately after sacrifice. Skin samples were cut using a template 4 mm wide by 20 mm long. Two skin samples, of identical width and length, were harvested from each mouse. The long axis of all samples coincided with the anterior-posterior direction of the mice. The thickness of each sample was determined using a micrometer at two consecutive locations along the middle 5-mm part of the skin specimens, and an average of the two measures was used for analysis. Approximately 7 mm of each end of the skin samples were subsequently allowed to air dry at room temperature, while keeping the middle 5-mm part moist by PBS-soaked gauze. Thereafter, the dried sample ends were glued to the uncoated aluminium endplates of the mechanical rig with cyanoacrylate glue. When the glue was hardened, the skin

samples and the endplates were attached to the mechanical test frame and submerged in a petri dish with PBS. Subsequently, the mechanical test frame was placed under a stereoscopic microscope (SMZ1000, Nikon, Tokyo, Japan) and the failure test was initiated. All failure tests were conducted with a constant plate-plate elongation velocity of 2.0 mm/min corresponding to 40% strain/min.

The microtensile mechanical rig was equipped with a 50-Newton load cell with 1% accuracy (Deben UK Ltd., Suffolk, UK.), a specimen chamber, and two specimen clamps driven by Maxon motor 118516 with 241062 encoder fitted that achieved and measured changes in grip displacement.

The cross-sectional area of the skin samples were calculated based on the measured width and thickness of the individual samples (width x thickness) on the assumption that the samples had a square cross-section. Sample stress was calculated as the tensile force (N) divided by the cross-sectional area (m^2) of the samples and reported in megapascal units (MPa). Peak stress was defined as the greatest magnitude of stress prior to tissue failure. All samples failed between the endplates of the mechanical rig, approximately in the middle of the specimen.

RESULTS

Generation of *Dse*-knockout mice. In order to functionally disrupt the *Dse* gene, a neomycin-resistance cassette was inserted after the ATG translational start in exon 2 (Fig. 1A). The resulting 6.3-kb targeting vector was electroporated into129/Sv embryonic stem cells. Out of 62 ES clones screened for homologous recombination

by Southern blot, ten clones contained the mutated allele (Fig. 1B). Three positive ES clones were injected into blastocysts, of which two yielded chimeric mice. *Dse*+/- mice were generated by mating chimeric male with C57BL/6 female. Breeding of the resulting heterozygous 129/Sv//C57BL/6 mice, i.e. with a mixed genetic background, resulted in *Dse*-deficient and wild-type littermates, which were analyzed in this report (Fig. 1C). The mice (n=198) were 18% *Dse* -/-, 33% *Dse* +/+ and 49% *Dse* +/-.

***Dse*-/- mice are smaller and have a kinked tail.** At birth *Dse*-/- mice were smaller with a 20-30% reduced body weight as compared to wild-type littermates (Fig. 2A and 2B). All *Dse*-/- pups had a tail with a kink that was not present after four weeks of age. At 80 days of age the *Dse*-deficient mice remained 5-10% shorter (crown-rump length) and 10% lighter (Fig. 2B). Adrenal gland, brain, intestines, kidney, lungs, and other major organs of 6-month-old *Dse*-deficient mice were necroscopically and histologically examined, and no gross changes were observed. Skin (see below) showed histological alterations. *Dse*-/- mice had reduced fertility; intercrosses of *Dse*-/- mice gave litters of 2-4 pups (9 litters), compared to 8-12 pups obtained from heterozygous or wild-type parents. Six *Dse*-/- mice were followed till 16 months of age and don't have increased mortality.

In *Dse*-/- mice DS-epimerase 1 expression is abolished and epimerase activity is reduced. DS-epi1 is highly expressed in spleen. A qRT-PCR product of the expected size was obtained from wild-type spleen ($C_t = 27$, or ΔC_t of 6.5 compared with the reference 18S rRNA gene) but was absent, even after 40 PCR cycles, in *Dse*-/- organ. Spleen was also analyzed for DS-epi1 protein expression by western

blot. Analysis of 100 μg of spleen lysates revealed a ~100 kDa band present in wild-type samples and absent in *Dse*-/- samples (Fig. 3A). This band co-migrated with the band derived from DS-epi1 overexpressed in 293HEK cells. To increase the sensitivity of the analysis, DS-epi1 was enriched from 5 mg of lysates by Red-Sepharose gel and western blotted. The ~100 kDa DS-epi1 band was reduced to about 50% in *Dse*+/- compared to wild-type, and was missing in *Dse*-/- spleens derived from two mice, each originating from two different ES clones. A less predominant band of ~78kDa was present only in the enriched sample from spleen and might represent a degradation product. Identical results were generated from lung tissue (data not shown). DS-epi 1 expression was similarly analyzed in skin fibroblasts derived from adult wild-type and *Dse*-/- mice (Fig. 3A). A single ~100 kDa band was detected in wild-type but not in the *Dse*-/- cells. Similar results were obtained from adult lung fibroblasts and mouse embryonic fibroblasts derived from wild-type and *Dse*-/- mice (data not shown). Epimerase activity was assayed in five organ lysates from 4-week-old mice, which showed a greatly diversified specific epimerase activity: skin released 1,170 dpm of tritium from the substrate/h/mg of protein, spleen 753, lung 466, kidney 127, and brain 41. The *Dse*+/- lysates contained activity that spanned 47 till 107% of the corresponding wild-type organs (Fig. 3B). *Dse*-/- spleen and kidney contained 4% of the activity compared to the wild-type samples, lung 18%, skin 35%, brain 86% (Fig. 3B). The remaining activity is most likely catalyzed by DS-epi2. Specific epimerase activity was 2,074 dpm/h/mg in wild-type adult skin fibroblasts, and decreased 35% in the corresponding *Dse*-/- cells.

The whole body-derived *Dse*-/- dermatan sulfate lacks iduronic acid blocks and has reduced amount of iduronic acid-2-sulfated-N-acetylgalactosamine-4-sulfated structures. To obtain a general picture of the alterations in CS/DS, GAG chains were ^{35}S-labeled *in vivo* and extracted from the entire mouse. Similar amounts of ^{35}S radioactivity were recovered in the CS/DS chains from mice of all three genotypes. Moreover, the size distribution of the ^{35}S-labeled CS/DS chains, as seen on gel permeation, was similar in the three genotypes (data not shown). Purified CS/DS chains were analyzed for the amount and distribution of iduronic acid by chondroitinase B and AC-I, which cleave GalNAc~IdoA and GalNAc~GlcA linkages, respectively. Digestion of wild-type chains by chondroitinase B yielded a disaccharide peak, derived from at least three contiguous IdoA-GalNac sequences in the native chain, amounting to 7.3% of the total radioactivity of the split products (Fig. 4A). Wild-type tetrasaccharides, derived from ~IdoA-GalNAc-GlcA-GalNAc~IdoA sequences in the native chains, amounted to 11.5%. The corresponding sample from the *Dse*-/- mouse showed 1% of the disaccharides (~ 7-fold reduction compared to wild-type), and 2.3% of the tetrasaccharides (~5-fold reduction). The sum of hexa-, octa-, and decasaccharide fractions, coming from ~IdoA-$(GalNAc\text{-}GlcA)_{n\ 2\text{-}4}$-GalNAc~IdoA sequences in the native chains, were a minor component both in the wild-type and *Dse*-/- samples and were very similar, amounting to 7.2% and 6.9%, respectively. The split product size distribution coming from wild-type and *Dse*+/- samples was almost superimposable. Disregarding the possible occurrence of nonsulfated disaccharide units, lacking radiolabel, calculations from the disaccharide till decasaccharide

fractions resulted in total IdoA content of 14.9% in wild-type, 16.8% in *Dse*+/- chains, and 3.4% in *Dse*-/- chains, which therefore have 23% remaining IdoA compared to wild-type (Fig 4B). Digestion by chondroitinase AC-I leaves unaffected structures constituted by adjacent $(IdoA\text{-}GalNAc)_n$ units. Wild-type mice produced such structures with more than 4 adjacent units, eluting the vast majority of them in the void volume of the column (Fig. 4C). These structures, called iduronic acid blocks, amounted to 19% of the total radioactivity in *Dse*+/+ chains, decreased to 15.1% in *Dse*+/-, and were missing in *Dse*-/- chains.

Dse+/+ and *Dse*-/- CS/DS chains were also cleaved by chondroitinase ABC, and the resulting disaccharides were separated by HPLC. The iduronic-2-sulfated-N-acetylgalactosamine-4-sulfated structures, recovered as ΔB after the analysis, were reduced by 85% in *Dse*-/- chains (Table I).

Skin decorin/biglycan- and versican-CS/DS *Dse*-/- chains contain less iduronic acid blocks and iduronic acid-2-sulfated-N-acetylgalactosamine-4-sulfated structures. ^{35}S-sulfate *in vivo* labeled versican and a mixture of decorin and biglycan were purified, and their CS/DS chains recovered. Either versican-derived chains or decorin/biglycan-derived chains were of comparable size, as shown by gel filtration, irrespective of the different genotypes (Fig. 5A). Chondroitinase B or AC-I digestion made it possible to determine the amount and distribution of iduronic acid along the chain, as outlined above. In skin decorin/biglycan-CS/DS iduronic acid content decreased from 67.1% in wild-type to 17.9% in *Dse*-/-, as calculated from the chondroitinase B split product distribution (Fig. 5B). The entire decrease of iduronic acid content could be

attributed to the 90% decrease of the iduronic acid blocks, which accounted for 58.2% of the total chain in wild-type and 5.6% in *Dse*-/- (Fig. 5C). Skin versican CS/DS wild-type chains contained 13.3% of iduronic acid, which decreased to 1.4% in *Dse*-/- (Fig. 5D). Iduronic acid blocks were 7.5% of the total wild-type chain and 0.6% of the *Dse*-/- chains (Fig. 5E).

Size distribution of decorin/biglycan-derived *Dse*+/+ iduronic acid blocks, obtained after chondroitinase AC-I digestion, was analyzed and the modal length value was 15 kDa, corresponding to approximately 30 disaccharide residues (Fig. 5F), as long as the intact, i.e. uncleaved, chain (Fig. 5A).

Furthermore, the iduronic-2-sulfated-N-acetylgalactosamine-4-sulfated structures were reduced by 70% in *Dse*-/- decorin/biglycan chains (Table I).

DS-epi1 deficiency alters skin morphology, collagen fibril ultrastructure, and skin tensile strength. Skin samples obtained from five *Dse*-/- mice contained sparser loose connective tissue in the hypodermal layer (Fig. 6 A-D). These structural changes did not alter the morphology or the numbers of hair follicles (wild-type = 33±10 hair follicles/tail cross-section, n=7; *Dse*-/- 29.5±4.5, n=8). The collagen content, as determined by hydroxyproline, was not significantly different in the skin of wild-type (20.8 ng hydroxyproline/mg wet weight, n=4, range=16.8-25.3) and *Dse*-deficient mice (18.6 ng hydroxyproline/mg wet weight, n=4, range=17.3-20.8). Immunostaining of decorin showed a similar staining pattern and indicate that the distribution and amount of decorin is similar in wild-type and *Dse*-deficient skin (Fig.6 E-G). Similarly, staining with an anti-biglycan antiserum showed no change in distribution or amount of biglycan (not shown).

Transmission electron microscopy (TEM) pictures were taken at different levels of dermis and hypodermis (Fig. 7A). Analysis of the skin collagen fibril ultrastructure by TEM showed a shift towards thicker fibrils in *Dse*-/- skin. The mean fibril diameter shifted from 60 nm in wild-type to 85 nm in *Dse*-/- skin. The differences in fibril diameter remain in dermal and hypodermal areas. In some *Dse*-/- hypodermal areas collagen fibrils were absent. This agrees with the observations by light microscopy (Fig. 6). On the other hand, *Dse*-/- tail tendons showed a minor shift towards thicker fibrils compared to the wild-type tendon, and most of the fibrils had the same diameter in both genotypes (Fig. 7B). There were no differences in collagen fibril diameter or morphology in the Achilles tendon (Fig. 7C). Fibril density did not change between the two genotypes (Table II).

We compared the relative amount of *Dse* mRNA in wild-type tissues by qRT-PCR. *Dse* mRNA was more abundant in skin than in the tendons, with spleen and lung having the highest amounts (Fig. 7D).

The altered collagen fibrils in the *Dse*-/- skin were accompanied by a decrease in mechanical strength (Fig. 8). The stress at failure was 5.86 ±1.88 MPa (n=5) in wild-type skin and 3.48±1.12 MPa (n=5) in *Dse*-/- skin, representing a 41% reduction.

Skin decorin/biglycan from wild-type and *Dse*-/- mice have differential effects on collagen fibril formation *in vitro*. To compare the biophysical properties of skin collagen from wild-type and *Dse*-/- mice, the collagen denaturation was analyzed in a differential scanning calorimeter. Skin from the *Dse*-/- mice denatures

more heterogeneously having two denaturation peaks at 60 and 62ºC, as compared to wild-type skin with only the 60ºC peak (Fig. 9A).

Decorin and biglycan are prominent CS/DS-proteoglycans in skin and have been shown to participate in collagen fibril formation (1). Decorin and biglycan were extracted from the skin of wild-type or *Dse*-/- adult mice with similar yields and obtained as a mixture containing 90-95% decorin. Both PGs migrated in a similar manner in SDS-PAGE (Fig. 9B), irrespective of the genotype. Similar amounts of decorin (Fig. 9C) and biglycan (data not shown) were present in the skin of the two genotypes. Acid-solubilized collagen was incubated in the presence of extracted decorin/biglycan preparations from the different genotypes. Differential scanning calorimeter analysis of the resulting collagen fibrils, which melted at around 50 ºC, showed a two-peak fibril-denaturation pattern in the presence of *Dse*-/- decorin/biglycan and a single peak after addition of wild-type decorin/biglycan (Fig. 9D), similar to the results obtained with intact skin. The denaturation of collagen monomers, occuring at 42ºC, was unaffected. We also investigated the kinetics of *in vitro* collagen fibril formation after addition of the decorin/biglycan preparations, using turbidometry. In this assay, decorin isolated from the skin of three wild-type mice all inhibited the formation of collagen fibrils (Fig. 9E). In contrast, decorin/biglycan isolated from the skin of three *Dse*-/- mice stimulated fibril formation. After removal of the CS/DS chains by chondroitinase ABC, all decorin/biglycan preparations inhibited fibril formation, regardless of genotype. These results demonstrate that the iduronic acid blocks in CS/DS chains carried by decorin/biglycan have a direct effect on collagen fibril formation.

DISCUSSION

Biosynthesis of CS/DS is a multistep process, requiring at least 22 enzymes directly involved in the assembly and modification of the chain, starting from the activated monosaccharides and the sulfate donor PAPS. Multi-enzyme complexes are thought to accomplish these coordinated and fast reactions. The final structure of CS/DS is subjected to different levels of regulation *in vivo*, which is still poorly understood despite all the enzymes having been cloned and studied *in vitro*. DS-epi1 is one of the two DS-epimerases converting glucuronic acid to iduronic acid (23,34). An *in vivo* model with ablated DS-epi1 can provide new insights into the biological roles of specific CS/DS structures and the regulation of the biosynthetic machinery.

DS-epi1 mRNA and protein were not detectable in *Dse*-/- mice. In adult animals DS-epi1 is the enzyme responsible for the majority of the epimerase activity in spleen, kidney, lung, and skin. The remaining activity in these tissues can most likely be attributed to DS-epi2. Adult brain, where the activity of DS-epi2 is predominant, is an exception. This is in agreement with mRNA expression data in brain, showing the highest expression of DS-epi2 and the lowest of DS-epi1 (13,27). Ds-epi1 deficiency results in a 77% reduction of iduronic acid in newly synthesized CS/DS by *Dse*-/- mice. Skin decorin/biglycan and versican contain 67% and 13% of iduronic acid in their wild-type chains, respectively; they were similarly

affected by ablation of Ds-epi1, which led to 73% and 89% reduction of iduronic acid, respectively. Clearly DS-epi1 plays a role in the modification of both proteoglycans, at least in skin. In wild-type skin decorin/biglycan the iduronic acid blocks, with a modal length value of 15 kDa, can comprise almost the entire chain. In *Dse*-/- mice skin only 10% of iduronic acid blocks remain in decorin/biglycan. On the other hand, isolated iduronic acid residues, i.e. surrounded by glucuronic acid, are not affected in skin decorin/biglycan. On the contrary, in skin versican and in the whole body CS/DS, probably being the latter sample predominantly composed of versican-type chains, both isolated iduronic acid and iduronic acid blocks are downregulated. Our report is the first showing that versican contains iduronic acid blocks, at least in skin.

Interestingly, *Dse*+/- mice have approximately half the amount of the enzyme, but still produce chains which are almost identical to the wild-type chains. Our data also show that decreased epimerization does not affect the length of the CS/DS chains, differently to the effect of CS4ST1 ablation (50). Disaccharide fingerprint of CS/DS chains showed that, as a consequence of the reduction of the iduronic acid blocks, also the disulfated structures in the native chains $(IdoA\text{-}2OS\text{-}GalNAC\text{-}4OS)_n$ are greatly reduced, both in the whole body CS/DS and in skin decorin/biglycan. Our results support previous findings that locate the position of these disulfated structures within the iduronic acid blocks (17,24). In summary, DS-epi1 is the main but not the only enzyme synthesizing iduronic acid blocks *in vivo*. The presented data confirm the results obtained in lung fibroblasts (34), and further suggest that differential level of expression of the two epimerases in the different tissues,

together with the expression of the 4-O-sulfotransferase D4ST (35), is a primary determinant of the amount and distribution of iduronic acid.

Dse-/- mice in a mixed 129/Sv//C57BL/6 genetic background were vital, without any gross organ alteration. This is different from the perinatal mortality of heparan sulfate (HS) epimerase-deficient mice, which lack kidneys and have altered lungs (21). This probably reflects a different role for iduronic acid in HS and CS/DS in embryo development and the fact that only one epimerase is present in HS biosynthesis. *Dse*-/- mice were smaller at birth, but grew normally. We can speculate that the maternal/fetal-derived placenta - an organ rich in DS and decorin (12) - might have heparin cofactor II-mediated thrombotic imbalance and/or altered ECM, and therefore could play a role in the retardation of intrauterine growth. An indication of a combined maternal and fetal contribution to the severity of the intrauterine phenotype is the reduced litter size generated by knock-out parents.

Many organs might be affected under close examination by the deficiency of DS-epi1, which is ubiquitously expressed, with the possible exception of brain where DS-epi2 is the predominant epimerase. Therefore it will be interesting to study if organs rich in DS-epi1 like spleen and kidney, despite a normal morphological appareance, present some functional defects. We initially analyzed the skin of *Dse*-deficient mice since this tissue showed histological changes under light microscope and has high content of dermatan sulfate. *Dse*-/- skin has a different histological appearance than wild-type skin and the hypodermal region contains a sparse connective tissue. This resembles the skin from decorin-deficient mice [Fig. 3C and 3D in (7)]. The skin morphology did not lead to any alterations in the amount of

collagen, as determined by hydroxyproline content. Light microscopic investigation of *Dse*-deficient tail tendon and Achilles tendons revealed no morphological abnormalities. Collagen fibrils in the skin of *Dse*-/- mice are thicker than those in the wild-type skin. Decorin is an abundant CS/DS proteoglycan in skin, binds to collagen and affects collagen fibril formation *in vitro* (38). The decorin (*Dcn*)- and *Dse*-deficient mice both have changes in skin collagen fibril structure (7). In *Dcn*-deficient skin the fibrils show irregular outlines and a larger variation in diameters as compared to wild-type. The mean fibril diameter in *Dcn*-deficient and wild-type skin is similar, whereas the *Dse*-deficient skin has collagen fibrils with an increased mean diameter of 85 nm, as compared to 60 nm in the wild-type. *Dcn*-deficient tail tendons have abnormal collagen fibrils, some larger than 600 nm, with multiple lateral fusions. In contrast, *Dse*-deficient tail and Achilles tendons were largely unaffected. The lack of tendon phenotype is likely due to the measured lower level of DS-epi1 mRNA in tendons compared to skin, and to a lower content of iduronic acid in tendons (4). The skin from *Dcn*- and *Dse*-deficient mice both have reduced tensile strength as a possible result of altered collagen fibril assembly. The stress at failure was reduced by 40% and 70% as compared to wild-type *in Dse*- and *Dcn*-deficient skin (7), respectively. In summary, *Dcn*-/- and *Dse*-/- skins have overlapping but not identical alterations in collagen structures. This can be explained considering the total ablation of the proteoglycan in *Dcn-/-*, as opposed to ablation of some of its functional components in *Dse*-/-. The *Dse*-deficient skin phenotype was not the result of an altered expression level of decorin or biglycan. In fact, the amount of decorin and biglycan in skin, as determined by western blot,

immunohistochemistry, and chemical quantification after extraction, indicated no change in the amount due to *Dse* ablation. This is different from the functionally defective galactosyl tranferase I, responsible for a variant of the Ehlers-Danlos syndrome, which leads to altered amount of decorin, both as proteoglycan and as non-glycanated core protein (42). Our results therefore suggest that the iduronic acid blocks carried by decorin chain have a role in determining the structure and mechanical properties of collagen. We obtained further support by using preparations containing predominantly decorin and minor amount of biglycan, isolated from wild-type and *Dse*-deficient mouse skin. The denaturation of collagen fibrils pre-formed in the presence of *Dse*-/- PGs shows two closely spaced melting temperatures in differential scanning calorimetry, while wild-type PGs resulted in a single melting temperature. These patterns of denaturation were reproduced with intact skin from wild-type and *Dse*-/- mice and indicate that the iduronic acid blocks of dermatan sulfate affect the biophysical property of collagen fibrils. We also used decorin/biglycan from the two genotypes in turbidometric measurements of collagen fibril formation. PGs from wild-type skin inhibited the fibril formation, whereas *Dse*-/- PGs promoted fibrillogenesis. These results suggest that IdoA blocks have a role in the fibril formation process, and agree with previously reported roles of the dermatan sulfate chain (39).

The interaction between antiparallel CS/DS chains of two decorin molecules has been proposed to contribute to the lateral growth of collagen fibrils (40). In a skin healing model and in skin development from embryonic stage till adulthood, longer decorin chains correlate with wider interfibrillar spacing (19,30). In the mentioned

skin healing model the longer chains contained fewer $(IdoA\text{-}2OS\text{-}GalNAC\text{-}4OS)_n$ structures and therefore presumably fewer iduronic acid blocks (20), and thinner fibrils were present. Therefore, the structural changes described in our study in skin decorin/biglycan CS/DS chains, which contain less iduronic acid but have similar length, are different from the changes described during development and healing.

Understanding the role of the CD/DS chains is complicated by their multiple potential interactions. In *Dse*-/- mice altered amount and/or distribution of iduronic acid-containing structures, thought to be important for CS/DS:CS/DS interaction (10), might lead to modified affinity of these CS/DS self-interactions. This in turn could explain the changes in the fibril structures. CS/DS chains have been shown to contribute to the binding of decorin to collagen I (29). Iduronic acid affects CS/DS chain flexibility, which often favors protein binding (8). *Dse*-/- chains might have altered conformation affecting collagen I/decorin binding and ultimately the growth of the fibrils. Alternatively, fibril surface-associated proteins like the FACIT-collagen XIV (2,9) might bind not optimally via decorin CS/DS to the growing fibril, affecting its structure. Finally, behaviour of cells in skin, for instance fibroblasts could be modified by altered DS chains.

In conclusion, our results indicate that decorin/biglycan iduronic acid blocks have a role in skin collagen fibril formation and in the biophysical characteristics and mechanical properties of the skin.

REFERENCES

1. **Ameye, L. and M. F. Young**. 2002. Mice deficient in small leucine-rich proteoglycans: novel in vivo models for osteoporosis, osteoarthritis, Ehlers-Danlos syndrome, muscular dystrophy, and corneal diseases. Glycobiology **12**:107R-116R.

2. **Ansorge, H. L., X. Meng, G. Zhang, G. Veit, M. Sun, J. F. Klement, D. P. Beason, L. J. Soslowsky, M. Koch, and D. E. Birk**. 2009. Type XIV Collagen Regulates Fibrillogenesis: PREMATURE COLLAGEN FIBRIL GROWTH AND TISSUE DYSFUNCTION IN NULL MICE. J. Biol. Chem. **284**:8427-8438.

3. **Bao, X., T. Muramatsu, and K. Sugahara**. 2005. Demonstration of the pleiotrophin-binding oligosaccharide sequences isolated from chondroitin sulfate/dermatan sulfate hybrid chains of embryonic pig brains. J. Biol. Chem. **280**:35318-35328.

4. **Cheng, F., D. Heinegard, A. Malmstrom, A. Schmidtchen, K. Yoshida, and L. A. Fransson**. 1994. Patterns of uronosyl epimerization and 4-/6-O-sulphation in chondroitin/dermatan sulphate from decorin and biglycan of various bovine tissues. Glycobiology **4**:685-696.

5. **Choi, H. U., T. L. Johnson, S. Pal, L. H. Tang, L. Rosenberg, and P. J. Neame**. 1989. Characterization of the dermatan sulfate proteoglycans, DS-PGI and DS-PGII, from bovine articular cartilage and skin isolated by octyl-sepharose chromatography. J. Biol. Chem. **264**:2876-2884.

6. **Coster, L., L. A. Fransson, J. Sheehan, I. A. Nieduszynski, and C. F. Phelps**. 1981. Self-association of dermatan sulphate proteoglycans from bovine sclera. Biochem. J. **197**:483-490.

7. **Danielson, K. G., H. Baribault, D. F. Holmes, H. Graham, K. E. Kadler, and R. V. Iozzo**. 1997. Targeted disruption of decorin leads to abnormal collagen fibril morphology and skin fragility. J. Cell Biol. **136**:729-743.

8. **Ferro, D. R., A. Provasoli, M. Ragazzi, B. Casu, G. Torri, V. Bossennec, B. Perly, P. Sinay, M. Petitou, and J. Choay**. 1990. Conformer populations of L-iduronic acid residues in glycosaminoglycan sequences. Carbohydr. Res. **195**:157-167.

9. **Font, B., E. ubert-Foucher, D. Goldschmidt, D. Eichenberger, and R. M. van der**. 1993. Binding of collagen XIV with the dermatan sulfate side chain of decorin. J. Biol. Chem. **268**:25015-25018.

10. **Fransson, L. A., L. Coster, A. Malmstrom, and J. K. Sheehan**. 1982. Self-association of scleral proteodermatan sulfate. Evidence for interaction via the dermatan sulfate side chains. J. Biol. Chem. **257**:6333-6338.

11. **Fransson, L. A. and L. Roden**. 1967. Structure of dermatan sulfate. II. Characterization of products obtained by hyaluronidase digestion of dermatan sulfate. J. Biol. Chem. **242**:4170-4175.

12. **Giri, T. K. and D. M. Tollefsen**. 2006. Placental dermatan sulfate: isolation, anticoagulant activity, and association with heparin cofactor II. Blood **107**:2753-2758.

13. **Goossens, D., S. Van Gestel, S. Claes, P. De Rijk, D. Souery, I. Massat, B. D. Van den, H. Backhovens, J. Mendlewicz, C. Van Broeckhoven, and J. Del Favero**. 2003. A novel CpG-associated brain-expressed candidate gene for chromosome 18q-linked bipolar disorder. Mol. Psychiatry **8**:83-89.

14. **Hannesson, H. H., A. Hagner-McWhirter, K. Tiedemann, U. Lindahl, and A. Malmstrom**. 1996. Biosynthesis of dermatan sulphate. Defructosylated Escherichia coli K4 capsular polysaccharide as a substrate for the D-glucuronyl C-5 epimerase, and an indication of a two-base reaction mechanism. Biochem J. **313 (Pt 2)**:589-596.

15. **Iozzo, R. V.** 1999. The biology of the small leucine-rich proteoglycans. Functional network of interactive proteins. J. Biol. Chem. **274**:18843-18846.

16. **Kalamajski, S., A. Aspberg, and A. Oldberg**. 2007. The decorin sequence SYIRIADTNIT binds collagen type I. J. Biol. Chem. **282**:16062-16067.

17. **Karamanos, N. K., P. Vanky, A. Syrokou, and A. Hjerpe**. 1995. Identity of dermatan and chondroitin sequences in dermatan sulfate chains determined by using fragmentation with chondroitinases and ion-pair high-performance liquid chromatography. Anal. Biochem. **225**:220-230.

18. **Kusche-Gullberg, M. and L. Kjellen**. 2003. Sulfotransferases in glycosaminoglycan biosynthesis. Curr. Opin. Struct. Biol. **13**:605-611.

19. **Kuwaba, K., M. Kobayashi, Y. Nomura, S. Irie, and Y. Koyama**. 2001. Elongated dermatan sulphate in post-inflammatory healing skin distributes among collagen fibrils separated by enlarged interfibrillar gaps. Biochem. J. **358**:157-163.

20. **Kuwaba, K., Y. Nomura, S. Irie, and Y. Koyama**. 1999. Temporal changes in disaccharide composition of dermatan sulfate in the skin after epicutaneous application of hapten. J. Dermatol. Sci. **19**:23-30.

21. **Li, J. P., F. Gong, A. Hagner-McWhirter, E. Forsberg, M. Abrink, R. Kisilevsky, X. Zhang, and U. Lindahl**. 2003. Targeted disruption of a murine glucuronyl C5-epimerase gene results in heparan sulfate lacking L-iduronic acid and in neonatal lethality. J. Biol. Chem. **278**:28363-28366.

22. **Liu, X., M. L. Yeh, J. L. Lewis, and Z. P. Luo**. 2005. Direct measurement of the rupture force of single pair of decorin interactions. Biochem. Biophys. Res. Commun. **338**:1342-1345.

23. **Maccarana, M., B. Olander, J. Malmstrom, K. Tiedemann, R. Aebersold, U. Lindahl, J. P. Li, and A. Malmstrom**. 2006. Biosynthesis of dermatan sulfate: chondroitin-glucuronate C5-epimerase is identical to SART2. J. Biol. Chem. **281**:11560-11568.

24. **Maimone, M. M. and D. M. Tollefsen**. 1991. Structure of a dermatan sulfate hexasaccharide that binds to heparin cofactor II with high affinity. J. Biol. Chem. **266**:14830.

25. **Malmstrom, A. and L. A. Fransson**. 1975. Biosynthesis of dermatan sulfate. I. Formation of L-iduronic acid residues. J. Biol. Chem. **250**:3419-3425.

26. **McBurney, M. W., L. C. Sutherland, C. N. Adra, B. Leclair, M. A. Rudnicki, and K. Jardine**. 1991. The mouse Pgk-1 gene promoter contains an upstream activator sequence. Nucleic Acids Res. **19**:5755-5761.

27. **Nakao, M., S. Shichijo, T. Imaizumi, Y. Inoue, K. Matsunaga, A. Yamada, M. Kikuchi, N. Tsuda, K. Ohta, S. Takamori, H. Yamana, H. Fujita, and K. Itoh**. 2000. Identification of a gene coding for a new squamous cell carcinoma antigen recognized by the CTL. J. Immunol. **164**:2565-2574.

28. **Nandini, C. D. and K. Sugahara**. 2006. Role of the sulfation pattern of chondroitin sulfate in its biological activities and in the binding of growth factors. Adv. Pharmacol. **53**:253-279.

29. **Nareyeck, G., D. G. Seidler, D. Troyer, J. Rauterberg, H. Kresse, and E. Schonherr**. 2004. Differential interactions of decorin and decorin mutants with type I and type VI collagens. Eur. J. Biochem. **271**:3389-3398.

30. **Nomura, Y.** 2006. Structural change in decorin with skin aging. Connect. Tissue Res. **47**:249-255.

31. **Obrink, B.** 1973. A study of the interactions between monomeric tropocollagen and glycosaminoglycans. Eur. J. Biochem. **33**:387-400.

32. **Oldberg, A., S. Kalamajski, A.V. Salnikov, L. Stuhr, M. Morgelin, R.K. Reed, N.E. Heldin, and K. Rubin.** 2007. Collagen-binding proteoglycan fibromodulin can determine stroma matrix structure and fluid balance in experimental carcinoma. Proc.Natl.Acad.Sci.U.S.A **104**: 13966-13971

33. **Osoegawa, K., M. Tateno, P. Y. Woon, E. Frengen, A. G. Mammoser, J. J. Catanese, Y. Hayashizaki, and P. J. de Jong**. 2000. Bacterial artificial

chromosome libraries for mouse sequencing and functional analysis. Genome Res. **10**:116-128.

34. **Pacheco, B., A. Malmstrom, and M. Maccarana**. 2009. Two dermatan sulfate epimerases form iduronic acid domains in dermatan sulfate. J. Biol. Chem. **284**:9788-9795.

35. **Pacheco, B., A. Malmstrom, and M. Maccarana**. 2009. Dermatan 4-O-sulfotransferase 1 is pivotal in the formation of iduronic acid blocks in dermatan sulfate. Glycobiology, *in press*

36. **Prabhakar, V. and R. Sasisekharan**. 2006. The biosynthesis and catabolism of galactosaminoglycans. Adv. Pharmacol. **53**:69-115.

37. **Rauch, U. and J. Kappler**. 2006. Chondroitin/Dermatan sulfates in the central nervous system: their structures and functions in health and disease. Adv. Pharmacol. **53**:337-356.

38. **Reed, C. C. and R. V. Iozzo**. 2002. The role of decorin in collagen fibrillogenesis and skin homeostasis. Glycoconj. J. **19**:249-255.

39. **Ruhland, C., E. Schonherr, H. Robenek, U. Hansen, R. V. Iozzo, P. Bruckner, and D. G. Seidler**. 2007. The glycosaminoglycan chain of decorin plays an important role in collagen fibril formation at the early stages of fibrillogenesis. FEBS J. **274**:4246-4255.

40. **Scott, J. E. and A. M. Thomlinson**. 1998. The structure of interfibrillar proteoglycan bridges (shape modules') in extracellular matrix of fibrous connective tissues and their stability in various chemical environments. J. Anat. **192 (Pt 3)**:391-405.

41. **Seidler, D. G., E. Breuer, K. J. Grande-Allen, V. C. Hascall, and H. Kresse**. 2002. Core protein dependence of epimerization of glucuronosyl residues in galactosaminoglycans. J. Biol. Chem. **277**:42409-42416.

42. **Seidler, D. G., M. Faiyaz-Ul-Haque, U. Hansen, G. W. Yip, S. H. Zaidi, A. S. Teebi, L. Kiesel, and M. Gotte**. 2006. Defective glycosylation of decorin and biglycan, altered collagen structure, and abnormal phenotype of the skin fibroblasts of an Ehlers-Danlos syndrome patient carrying the novel Arg270Cys substitution in galactosyltransferase I (beta4GalT-7). J. Mol. Med. **84**:583-594.

43. **Shively, J. E. and H. E. Conrad**. 1976. Formation of anhydrosugars in the chemical depolymerization of heparin. Biochemistry **15**:3932-3942.

44. **Sugahara, K. and T. Mikami**. 2007. Chondroitin/dermatan sulfate in the central nervous system. Curr. Opin. Struct. Biol. **17**:536-545.

45. **Svensson, L., A. Aszodi, F. P. Reinholt, R. Fassler, D. Heinegard, and A. Oldberg**. 1999. Fibromodulin-null mice have abnormal collagen fibrils, tissue organization, and altered lumican deposition in tendon. J. Biol. Chem. **274**:9636-9647.

46. **Taylor, K. R., J. A. Rudisill, and R. L. Gallo**. 2005. Structural and sequence motifs in dermatan sulfate for promoting fibroblast growth factor-2 (FGF-2) and FGF-7 activity. J. Biol. Chem. **280**:5300-5306.

47. **Tiedemann, K., T. Larsson, D. Heinegard, and A. Malmstrom**. 2001. The glucuronyl C5-epimerase activity is the limiting factor in the dermatan sulfate biosynthesis. Arch. Biochem. Biophys. **391**:65-71.

48. **Tollefsen, D. M.** 2007. Heparin cofactor II modulates the response to vascular injury. Arterioscler. Thromb. Vasc. Biol. **27**:454-460.

49. **Trowbridge, J. M. and R. L. Gallo**. 2002. Dermatan sulfate: new functions from an old glycosaminoglycan. Glycobiology **12**:117R-125R.

50. **Uyama, T., M. Ishida, T. Izumikawa, E. Trybala, F. Tufaro, T. Bergstrom, K. Sugahara, and H. Kitagawa**. 2006. Chondroitin 4-O-sulfotransferase-1 regulates E disaccharide expression of chondroitin sulfate required for herpes simplex virus infectivity. J. Biol. Chem. **281**:38668-38674.

TABLE I.

Disaccharide composition of *Dse*+/+ and *Dse*-/- CS/DS chains.

The CS/DS preparations were digested with chondroitinase ABC and the resulting disaccharides analyzed by anion-exchange HPLC.

	Whole body		Skin	
	Total CS/DS [a]		Decorin/biglycan-derived[b]	
	Dse+/+	*Dse*-/-	*Dse*+/+	*Dse*-/-
	mol%			
ΔO unit, ΔHexA-GalNAc	n.a. [c]	n.a.	1.0	1.3
ΔA unit, ΔHexA-GalNAc4S	86.6	86.6	89.5	95.1
ΔC unit, ΔHexA-GalNAc6S	7.6	10.1	0.6	0.8
ΔB unit, ΔHexA2S-GalNAc4S	3.4	0.5	9.0	2.7
ΔE unit, ΔHexA-GalNAc4S6S	1.7	1.7	n.d. [d]	n.d.
ΔD unit, ΔHexA2S-GalNAc6S	0.7	1.1	n.d.	n.d.

[a] *In vivo* labeled CS/DS chains were prepared from the whole mouse, as described under "Experimental procedures".

[b] Unlabeled CS/DS chains were prepared from skin decorin/biglycan from 4-month-old mice. The disaccharides obtained after chondroitinase ABC digestion were labeled with the reducing reagent NaB^3H_4.

[c] n.a., not applicable

[d] n.d., none detected (less than 0.1%)

TABLE II.

Fibril density calculated from TEM images.

	Fibril density
	(% area occupied by fibrils in the TEM images)±SE
Wild-type dermis	72 ± 5
Dse-/- dermis	68 ± 7
Wild-type hypodermis	62 ± 5
Dse-/- hypodermis	60 ± 8
Wild-type tail tendon	75 ± 7
Dse-/- tail tendon	88 ± 8
Wild-type Achilles	74 ± 8
Dse-/- Achilles	77 ± 10

FOOTNOTES

1) The abbreviations used are: CS, chondroitin sulfate; Δunits, 4,5-unsaturated hexuronic acid residues, originating from the degradative process catalyzed by chondroitinase ABC; DS, dermatan sulfate; DS-epi1, DS-epimerase 1; DS-epi2, DS-epimerase 2; GlcA, glucuronic acid; GalNAc, N-acetyl-galactosamine; HS, heparan sulfate; IdoA, iduronic acid; MES, 4-morpholineethanesulfonic acid;

2) This work was supported by grants from the Swedish Science Research Council, the Medical Faculty of Lund University, the Albert Österlund Foundation, the Greta and Johan Kock Foundation, Polysackaridforskning AB, and the Tissue in Motion Medical Faculty Program.

3) The authors are grateful to Ragnar Mattsson - Lund Transgenic Core Facility - for the help in generating the knock-out mice and for precious advices, and to Ricardo Feinstein – National Veterinary Institute, Uppsala, Sweden – for the help in histological examinations.

FIGURE LEGENDS

FIG.1. Targeted disruption of the *Dse* gene.

(A) Schematic view of the *Dse* genomic structure (*first line*). Restriction enzyme map of the targeted *Dse* locus in exon 2 (*second line*); the location of the PCR product obtained from the wild-type allele is indicated. Targeting vector (*third line*); the location of the PCR product obtained from the mutated allele is indicated. The origin of the 6.3 and 4.8 kb NcoI fragments and the location of the common probe is shown in the *last two lanes*. (B) Southern blot of DNA isolated from ES cells. (C) PCR genotyping of the mice.

FIG. 2. Macroscopic appearance of the *Dse*-/- mice.

(A) *Dse*-/- newborn. *Arrow* points to the kinked tail. (B) Eight wild-type and *Dse*-/- males were weighed (± 2 S.D.). Similarly, female *Dse*-/- mice were smaller than wild-type mice (data not shown).

FIG. 3. DS-epi1 expression and epimerase activity in *Dse*-/- mice.

(A) Left gel: spleen homogenates were directly western blotted (100 μg protein applied) or DS-epi1 was enriched by Red-Sepharose, starting from 5 mg of initial lysates. *Central gel*: 20 μg of lysates from control or DS-epi1-overexpressing 293HEK cells. *Right gel*: 20 μg of lysates from adult skin primary fibroblast from *Dse*+/+ and *Dse*-/- mice. Membranes were probed with anti-Ds-epi1 antibody. (B) Equal amount of protein for each organ, irrespective to the genotype of origin, was

assayed for epimerase activity. Values (± 2 S.D. of triplicates) are reported as percent of specific epimerase activity referred to the wild-type organ. *Empty bars*, *Dse*+/-; *black bars*, *Dse*-/-. As example, the wild-type skin homogenates released 3,067 dpm of tritium from the labeled substrate during 20 h incubation.

FIG. 4. Analysis of *Dse*-/- CS/DS present in the whole body.

Ten-day-old pups were *in vivo* ^{35}S labeled and CS/DS was purified from the whole body. Chains were cleaved with (A) chondroitinase B or (C) chondroitinase AC-I. Split products were separated on the size-permeation Superdex Peptide column. Elution positions of di-, tetra-, hexa-, octa- and decasaccharides are indicated by *arrows*. AC-I-resistant iduronic acid blocks are shown. *Triangles*, *Dse*+/+; *squares*, *Dse*+/-; *circles*, *Dse*-/-. (B) Proportion of iduronic acid residues in the CS/DS chains, as calculated from (A).

FIG. 5. Analysis of *Dse*-/- skin decorin/biglycan- and versican-CS/DS chains.

Ten-day-old pups were *in vivo* ^{35}S labeled. Skin decorin/biglycan and versican were isolated and (A) their CS/DS chains analyzed by size-permeation on a Superose 6 column, run in 0.2 M NH_4HCO_3. Heparins of different molecular weight were used as markers. *Filled triangles*, wild-type decorin/biglycan chains; *empty triangles*, *Dse*-/- decorin/biglycan chains; *filled squares*, wild-type versican chains; *empty squares*, *Dse*-/- versican chains. (B-E) CS/DS chains were cleaved by chondroitinase B and AC-I, as indicated. Split products were separated as in Fig. 4. *Squares*, *Dse*+/+; *triangles*, *Dse*+/-; *circles*, *Dse*-/-. (F) Wild-type decorin/biglycan-

derived iduronic acid blocks, as obtained after chondroitinase AC-I and pooled as indicated in (C), were analyzed by size-permeation on a Superose 6 column, run in 1 M NaCl.

FIG. 6. Skin morphology and immunohistochemistry.

Tail skin (A-B) stained with Chromotrope 2R and visualized with light microscope or (C-D) stained with Sirius Red and visualized with polarized light. Sparser loose connective tissue appears in the hypodermis of *Dse-/-* (*arrow*). Bar = 100 μm. D = dermis; E = epidermis; H = hair follicles; T = tendons. (E-F) Histoimmunological detection of decorin. (G) Pre-immune serum control.

FIG. 7. Ultrastructure analysis of collagen fibrils in skin, tail tendon, and Achilles tendon.

Right panels, skin (A), tail tendon (B), Achilles tendon (C) were examined by electron microscopy. *Left panels (A-C)*, diameters of 1,000 fibrils from each source were measured and presented in histograms. *Solid bars*, wild-type; *open bars*, *Dse*-/-. (D) Quantitive RT-PCR of *Dse* mRNA from different wild-type tissues. Values (± 2 S.D. of triplicates) are normalized for spleen mRNA.

FIG. 8. Biomechanics of skin.

Stress at failure was measured by applying force to skin samples and measuring the stress at which the skin ruptured. Duplicate samples from five mice of each genotype were measured. Bars indicate mean values; P = 0.018.

FIG. 9. Biophysical properties of *Dse*-/- skin and effect of skin decorin/biglycan on collagen fibril formation *in vitro*.

(A) Differential scanning calorimetry of intact skin. Skin samples from 3-month-old mice were immersed in PBS in a calorimetric cell and heated over a temperature range of 30-90 ºC. Thermograms (no peaks after 70ºC) were normalized for buffer blank run without skin. (B) 500 ng of extracted decorin/biglycan from adult skin were applied to SDS-PAGE, and stained with Blue G Colloidal solution. (C) Proteoglycans were extracted from identical amount (fresh weight) of tail skin of 4-month-old mice. PGs were purified on anion exchange DE52 column and identical volumes of the eluates were western blotted and stained with anti-decorin antibody. (D) Differential scanning calorimetry of *in vitro* formed collagen fibrils. Prior to calorimetry, 500 μg acid-solubilized collagen was incubated for 4 h at 37ºC with addition of 10 μg wild-type or *Dse*-/- decorin/biglycan extracts from skin (one preparation is shown in (B)). Collagen fibrils were then heated in the calorimeter over a temperature range of 30-60ºC. Thermograms are normalized for buffer blank run without collagen. (E) Turbidometric measurements of *in vitro* collagen fibrillization. 50 μg acid-solubilized collagen was mixed with 1 μg decorin/biglycan extracts, either pre-treated or non-treated with chondroitinase ABC. The samples were then incubated at 37ºC in a spectrophotometer and readings of turbidity were taken every 4 min and plotted.

Fig. 1

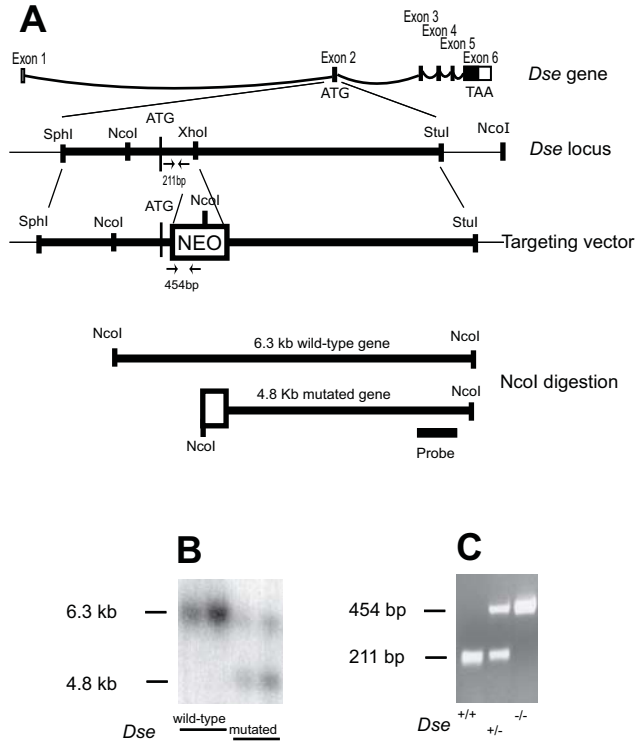
A
Exon 1
Exon 2
Exon 3
Exon 4
Exon 5
Exon 6
ATG
TAA
Dse gene
SphI
NcoI
ATG
XhoI
StuI
NcoI
Dse locus
211bp
NcoI
NEO
Targeting vector
454bp
6.3 kb wild-type gene
4.8 Kb mutated gene
NcoI digestion
Probe
B
6.3 kb
4.8 kb
Dse
wild-type
mutated
C
454 bp
211 bp
Dse
+/+
+/-
-/-

Fig. 2

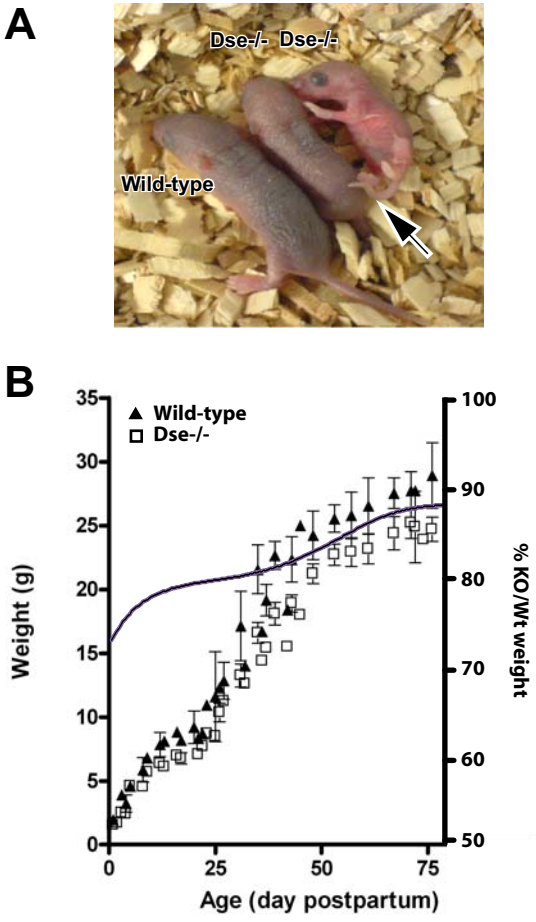
A
Dse-/- Dse-/-
Wild-type
B
Wild-type
Dse-/-
Weight (g)
% KO/Wt weight
Age (day postpartum)
0
5
10
15
20
25
30
35
50
60
70
80
90
100
0
25
50
75

Fig. 3

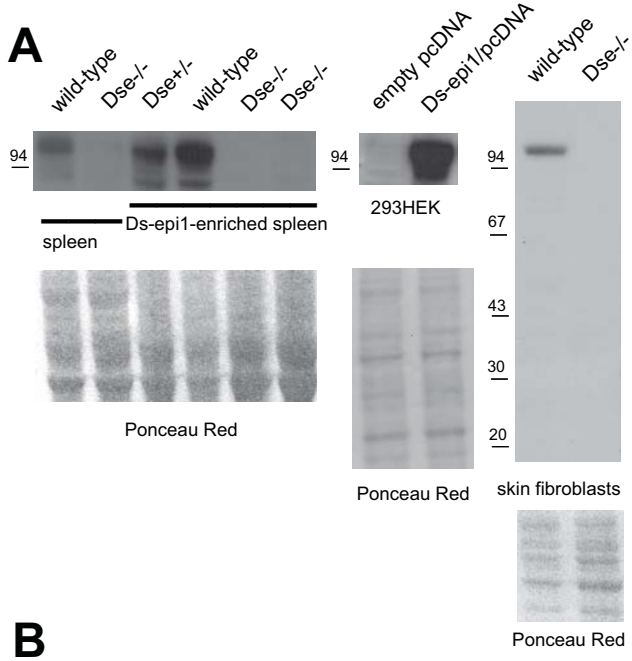
A
wild-type
Dse-/-
Dse+/-
wild-type
Dse-/-
Dse-/-
94
spleen
Ds-epi1-enriched spleen
Ponceau Red
empty pcDNA
Ds-epi1/pcDNA
94
293HEK
Ponceau Red
wild-type
Dse-/-
94
67
43
30
20
skin fibroblasts
Ponceau Red
B
Specific epimerase activity
(Percent of wild-type)
110
100
90
80
70
60
50
40
30
20
10
0
skin
spleen
lung
kidney
brain

Fig. 4

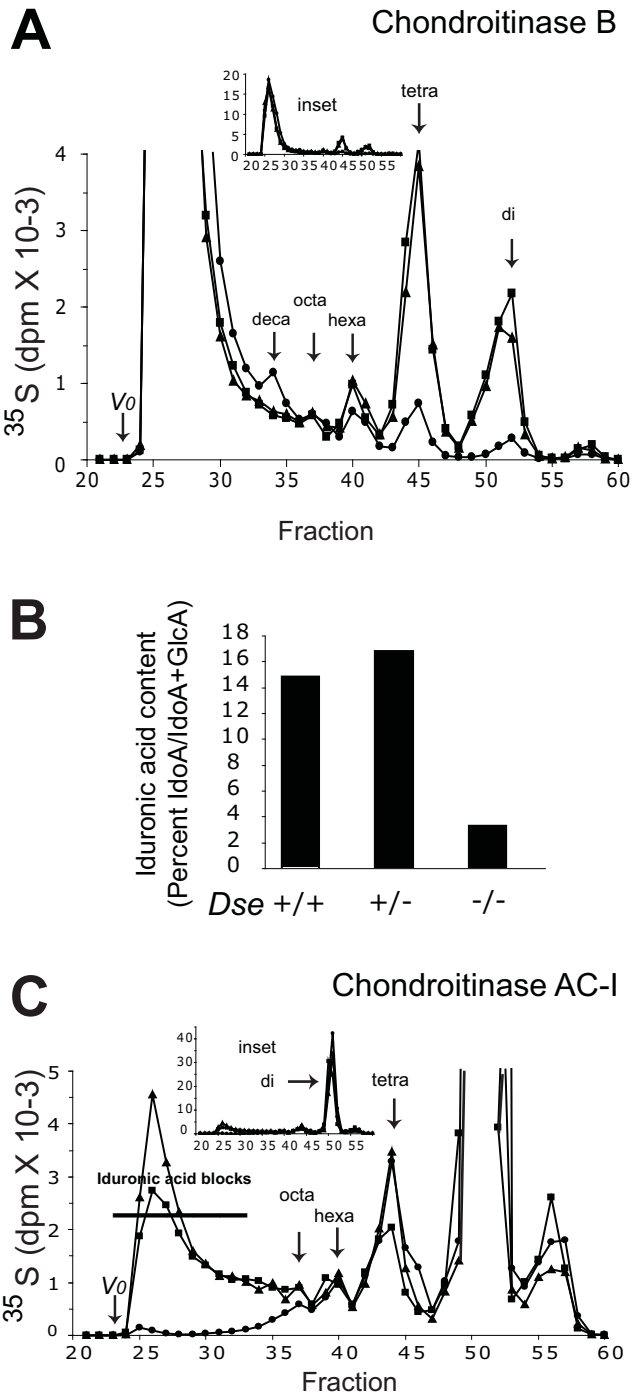
A
Chondroitinase B
inset
tetra
di
deca
octa
hexa
V0
35S (dpm X 10-3)
Fraction
B
Iduronic acid content
(Percent IdoA/IdoA+GlcA)
Dse +/+
+/-
-/-
C
Chondroitinase AC-I
inset
di
tetra
Iduronic acid blocks
octa
hexa
V0
35S (dpm X 10-3)
Fraction

Fig. 5

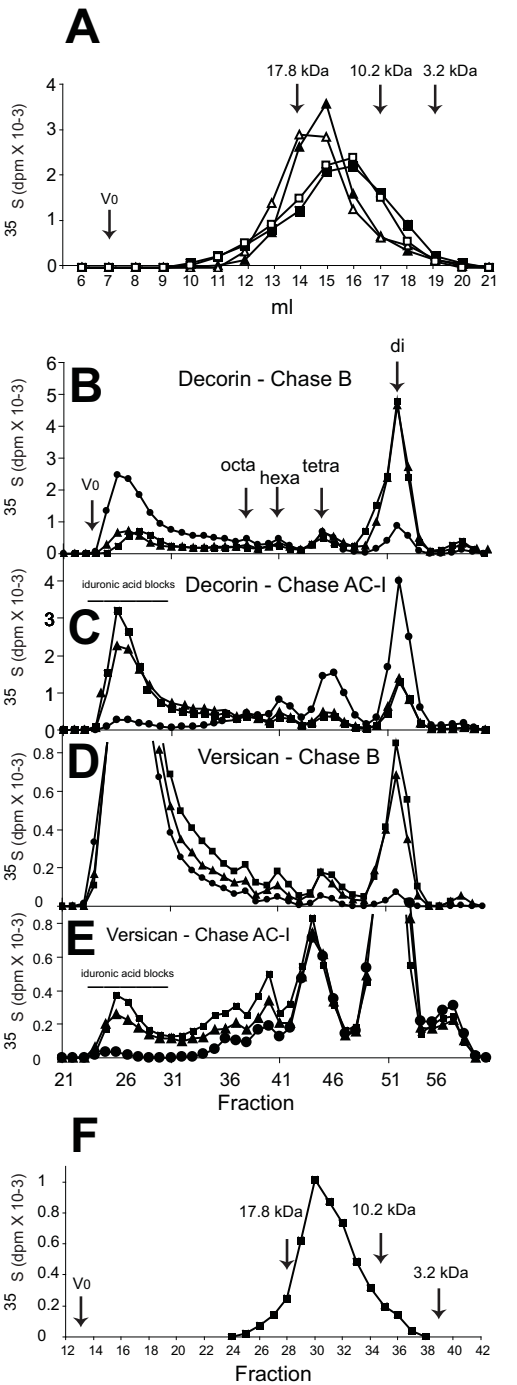
A
17.8 kDa
10.2 kDa
3.2 kDa
V0
35 S (dpm X 10-3)
ml
B
Decorin - Chase B
di
octa
hexa
tetra
C
iduronic acid blocks
Decorin - Chase AC-I
D
Versican - Chase B
E
Versican - Chase AC-I
Fraction
F

Figure 6

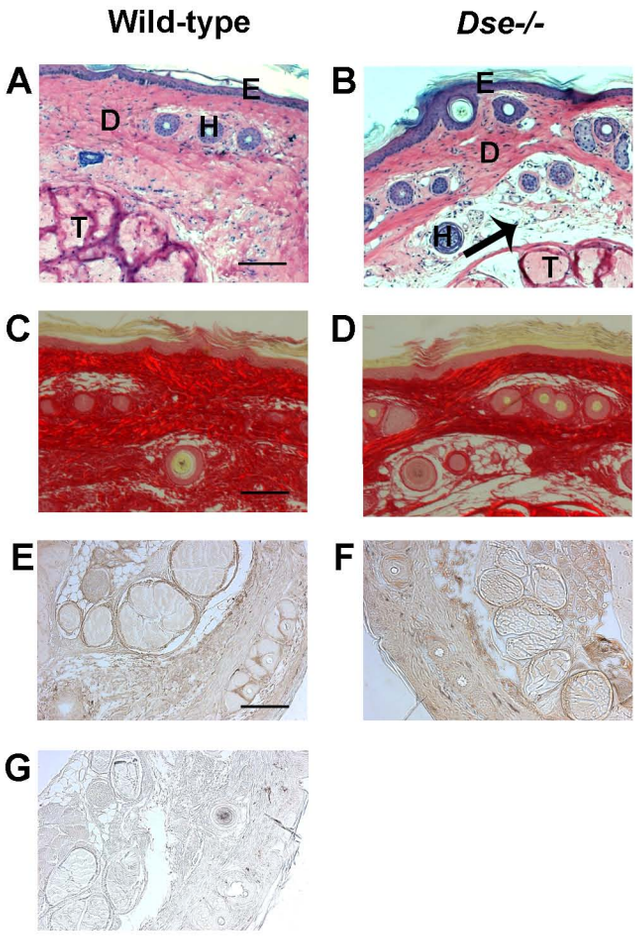

Figure 7

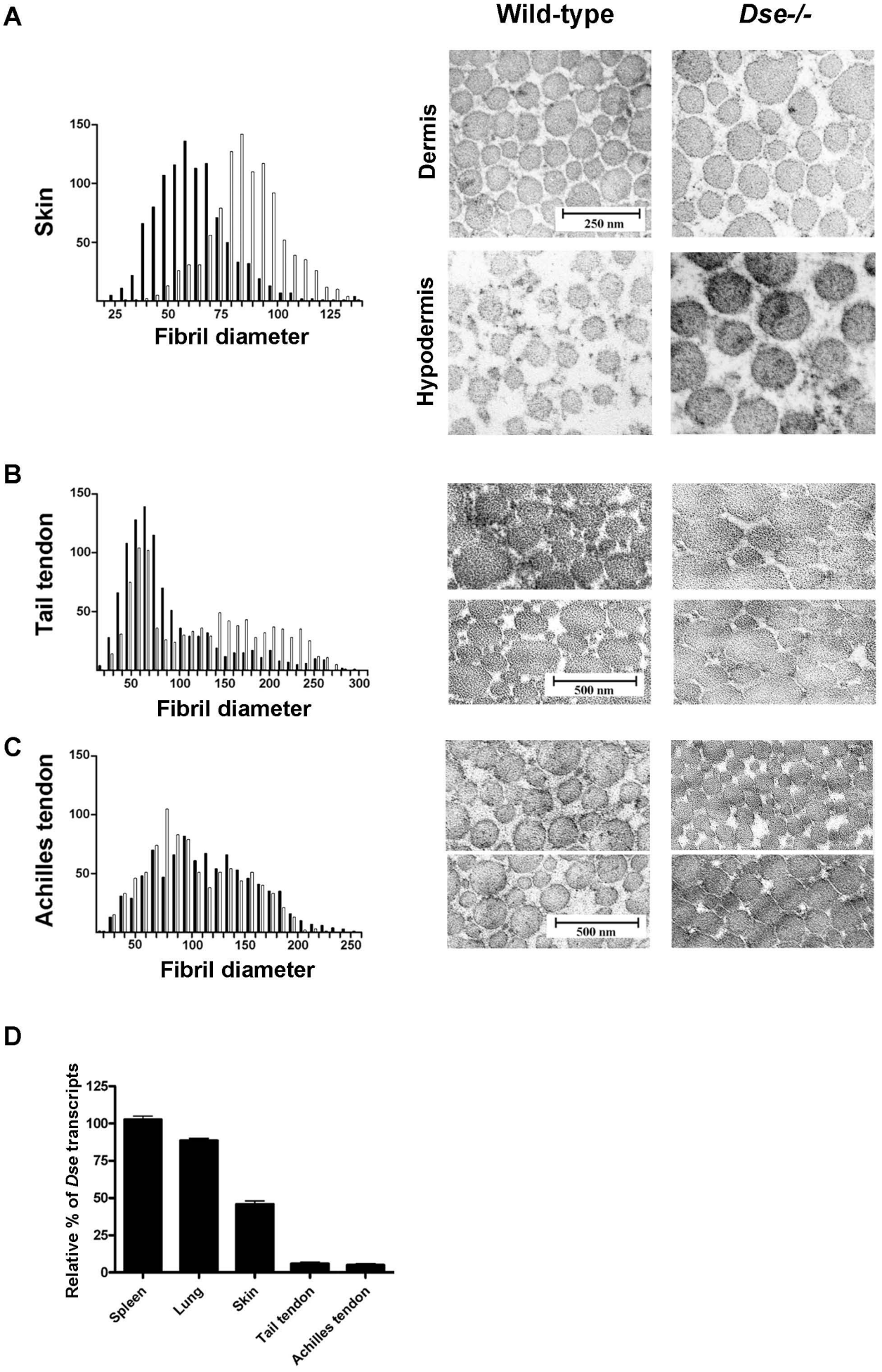
A
Wild-type
Dse-/-
Skin
Fibril diameter
Dermis
Hypodermis
250 nm
B
Tail tendon
Fibril diameter
500 nm
C
Achilles tendon
Fibril diameter
500 nm
D
Relative % of Dse transcripts
Spleen
Lung
Skin
Tail tendon
Achilles tendon

Figure 8

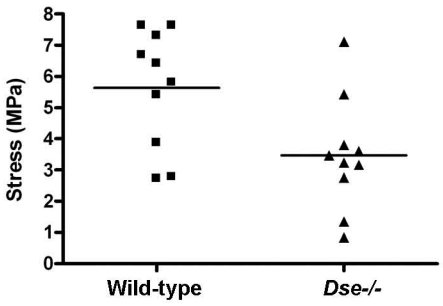

Figure 9

A

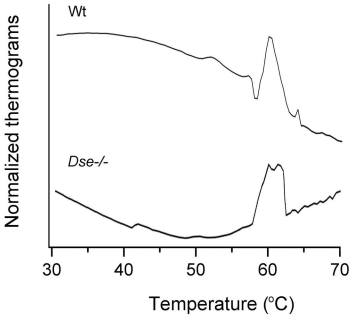

B

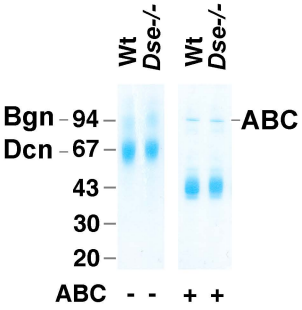

C

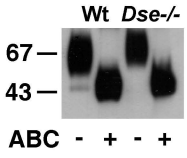

D

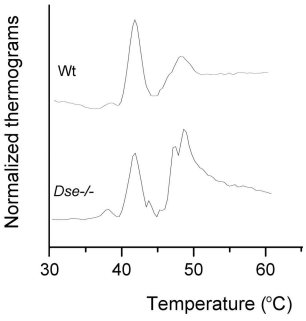

E